# Making corrections to your proof

Please follow these instructions to mark changes or add notes to your proof. You can use Adobe Acrobat Reader (download the most recent version from **https://get.adobe.com**) or an open source PDF annotator.

For Adobe Reader, the tools you need to use are contained in **Annotations** in the **Comment** toolbar. You can also right-click on the text for several options. The most useful tools have been highlighted here. If you cannot make the desired change with the tools, please insert a sticky note describing the correction.

Please ensure all changes are visible via the 'Comments List' in the annotated PDF so that your corrections are not missed.

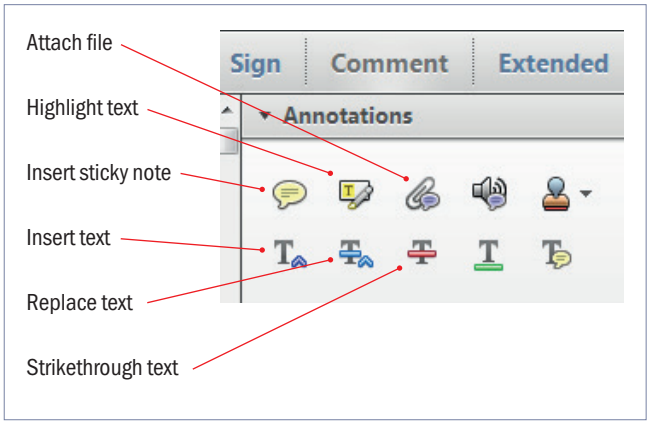


**Do not attempt to directly edit the PDF file as changes will not be visible.**

### Replacing text

To replace text, highlight what you want to change then press the replace text icon, or right-click and press 'Add Note to Replace Text', then insert your text in the pop up box. Highlight the text and right click to style in bold, italic, superscript or subscript.

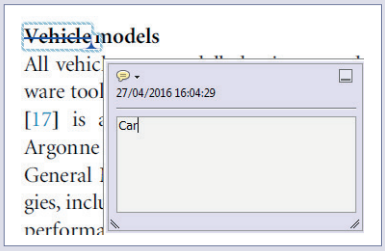


### Inserting text

Place your cursor where you want to insert text, then press the insert text icon, or right-click and press 'Insert Text at Cursor', then insert your text in the pop up box. Highlight the text and right click to style in bold, italic, superscript or subscript.

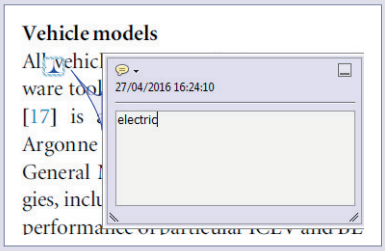


### Deleting text

To delete text, highlight what you want to remove then press the strikethrough icon, or right-click and press 'Strikethrough Text'.

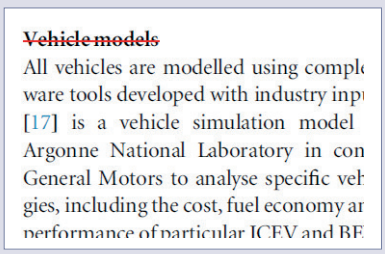


### Highlighting text

To highlight text, with the cursor highlight the selected text then press the highlight text icon, or right-click and press 'Highlight text'. If you double click on this highlighted text you can add a comment.

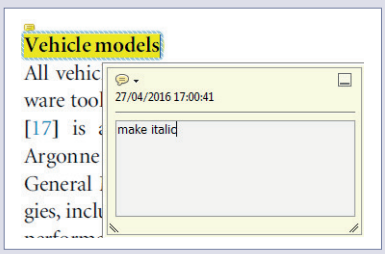

# QUERY FORM

JOURNAL: Japanese Journal of Applied Physics

AUTHOR: Y. Cai et al.

TITLE: Effect of surface treatment on electrical properties of GaN metal–insulator–semiconductor devices with $Al_2O_3$ gate dielectric

ARTICLE ID: ab7863

---

Your article has been processed in line with the journal style. Your changes will be reviewed by the Production Editor, and any amendments that do not comply with journal style or grammatical correctness will not be applied and will not appear in the published article.

The layout of this article has not yet been finalized. Therefore this proof may contain columns that are not fully balanced/ matched or overlapping text in inline equations; these issues will be resolved once the final corrections have been incorporated.

Please check that the **names of all authors as displayed in the proof are correct**, and that all **authors are linked to the correct affiliations**. Please also confirm that the correct corresponding author has been indicated. **Note that this is your last opportunity to review and amend this information before your article is published**.

If an explicit acknowledgment of funding is required, please ensure that it is indicated in your article. If you already have an Acknowledgments section, please check that the information there is complete and correct.

---

Please check that the funding information below is correct for inclusion in the article metadata.
Suzhou Industrial Park Initiative Platform Development for Suzhou Municipal Key Lab for New Energy Technology: RR0140; the Key Program Special Fund in XJTLU: KSF-A-05; Suzhou Science and Technology program: SYG201728.

We have been provided with ORCID iDs for the authors as below. Please confirm whether the numbers are correct.
Yutao Cai 0000-0002-2151-9325
Ruize Sun 0000-0003-1884-7114

**Page 1**

---

Q1
Please check the edits made to the sentence “After organic…”.

**Page 2**

---

Q2
Please confirm whether the hyphens in Fig. 1 can be replaced with en dashes, as per JSAP style.

**Page 3**

---

Q3
Please confirm whether the following changes can be made in Fig. 3: italicize C and V (voltage, not volts), use the format nF $cm^{-2}$ instead, and leave a space between values and units.

**Page 6**

---

Q4
Please confirm whether the following changes can be made in Fig. 4: italicize D and E, add a space before each opening parenthesis, and replace the hyphens with a minus sign or en dash.

**Page 6**

Q5
Please confirm whether the following changes can be made in Figs. 5 and 6: italicize I and V (voltage, not volts) and use the format mA $mm^{-1}$ instead.

**Page 7**

Q6
Please confirm whether the following changes can be made in Fig. 7: italicize V (voltage, not volts) and add a space before each opening parenthesis.

**Page 8**

Q7
Please provide updated details for reference [27] if available.

Japanese Journal of Applied Physics **00**, 000000 (2020) **REGULAR PAPER**
https://doi.org/**10.35848/1347-4065/ab7863**

# Effect of surface treatment on electrical properties of GaN metal–insulator–semiconductor devices with $Al_2O_3$ gate dielectric

Yutao Cai[1,2], Wen Liu[1,2], Miao Cui[1,2], Ruize Sun[3], Yung C. Liang[3], Huiqing Wen[1,2], Li Yang[4], Siti N. Supardan[2], Ivona Z. Mitrovic[2], Stephen Taylor[2], Paul R. Chalker[2], and Cezhou Zhao[1,2*]

[1]*Department of Electrical and Electronic Engineering, Xi'an Jiaotong–Liverpool University, Suzhou, People's Republic of China*
[2]*Department of Electrical Engineering and Electronics, University of Liverpool, Liverpool, United Kingdom*
[3]*Department of Electrical and Computer Engineering, the National University of Singapore, Singapore, Singapore*
[4]*Department of Chemistry, Xi'an Jiaotong–Liverpool University, Suzhou, People's Republic of China*

*E-mail: cezhou.zhao@xjtlu.edu.cn

Received November 20, 2019; revised February 16, 2020; accepted February 20, 2020; published online MM DD, 2020

This research proposes an economical and effective method of 1-octadecanethiol (ODT) treatment on GaN surfaces prior to $Al_2O_3$ gate dielectric deposition. GaN-based metal–insulator–semiconductor (MIS) devices treated by HCl, $O_2$ plasma and ODT are demonstrated. ODT treatment was found to be capable of suppressing native oxide and also of passivating the GaN surface effectively; hence the interface quality of the device considerably improved. The interface trap density of $Al_2O_3$/GaN was calculated to be around $3.0 \times 10^{12}\,cm^{-2}\,eV^{-1}$ for devices with ODT treatment, which is a relatively low value for GaN-based MIS devices with $Al_2O_3$ as the gate dielectric. Moreover, there was an improvement in the gate control characteristics of MIS-HEMTs fabricated with ODT treatment. © 2020 The Japan Society of Applied Physics

## 1. Introduction

AlGaN/GaN high electron mobility transistors (HEMTs) have superior properties for power electronics applications, such as high saturation velocity, high electron mobility, and good thermal conductivity and stability. However, AlGaN/GaN HEMTs suffer from large gate leakage currents due to a Schottky-gate contact.[1)] By replacing the Schottky-gate contact with a metal–insulator–semiconductor (MIS) structure, gate leakage currents can be suppressed significantly. High-$k$ dielectrics, such as $Al_2O_3$,[2)] $HfO_2$,[3)] $CeO_2$[4)] and $ZrO_2$,[5)] have been considered for MIS gate structures. The gate dielectric material should exhibit wide-band offsets to GaN in order to form a barrier for both electrons and holes. $Al_2O_3$ with large conduction and valence band offsets (2.1 eV and 3.4 eV respectively) to GaN[6)] and a high relative permittivity ($\sim$9)[7)] was chosen in this study. However, a high interface trap density of $\sim 1 \times 10^{13}\,cm^{-2}\,eV^{-1}$ at the $Al_2O_3$/GaN interface has been reported.[8)] This poor interface quality has been associated with native gallium oxide and dangling bonds on the GaN surface,[9)] resulting in large leakage currents and threshold voltage instability.

In order to reduce the interface-state density, treatments have been suggested as critical procedures to remove native oxide on GaN or to passivate the GaN surface prior to dielectric deposition. Surface cleaning with HCl[10)] or HF[11)] is commonly used to eliminate native oxide, but the exposed GaN surface suffers from re-oxidation before dielectric deposition. Sulfide-based passivation schemes, such as aqueous $(NH_4)_2S$ solution, are capable of protecting the GaN surface from immediate re-oxidation by forming Ga–S bonds.[12)] However, metal contamination of the $(NH_4)_2S$ solution and the limited stability of $(NH_4)_2S$ passivation during the fabrication processes[13)] are two limitations which might be detrimental to device performance. In contrast, a recent study[14)] reported that surface preparation using a sacrificial 1-octadecanethiol (ODT) self-assembled monolayer (SAM) can protect insulator/GaAs interfaces from interfacial oxides. Surface passivation by ODT SAMs can improve sulfide passivation stability in an air ambient environment.[15)] In addition, studies have reported that oxidation of the GaN surface is able to fill up the Ga dangling bonds, and form high-quality gallium oxides on the GaN surface.[16)] Among these oxidation methods, the oxygen plasma technique has been found to be an effective approach to passivate dangling bonds and remove possible carbon contamination on the GaN surface.[17)] Therefore, both removal of native oxide on the GaN surface and passivation of the GaN surface by Ga–S and Ga–O bonds are regarded as effective methods to reduce interface states.

In this paper, a low-cost method of ODT treatment is proposed to improve the $Al_2O_3$/GaN interface quality. The electrical characteristics of MIS devices, with $Al_2O_3$ as the gate dielectric deposited by atomic layer deposition (ALD), will be studied. Comparisons will be made between samples without any treatment and with HCl, oxygen plasma and ODT treatments prior to gate dielectric deposition.

## 2. Experimental methods

The investigated GaN-based material stack consisted of a 1 nm undoped GaN cap layer, a 22-nm-thick $Al_{0.25}Ga_{0.75}N$ barrier layer, a 0.33 $\mu$m GaN channel layer, and a 5.4 $\mu$m highly resistive GaN buffer on a Si substrate. Firstly, Au-free source and drain electrodes were formed by e-beam evaporation of Ti/Al/Ti/TiN (25/125/45/55 nm) patterned by photolithography and a lift-off technology, and annealed at 840 °C in ambient $N_2$ for 40 s by rapid thermal annealing. After the formation of ohmic contact, a mesa isolation region was formed by $BCl_3/Cl_2$ gas reactive-ion etching. After organic cleaning processes, sample A was set aside without any treatment. Samples B, C and D were treated in 2 M HCl solution at RT for 5 min to remove native oxide. In addition, sample C was subjected to $O_2$ plasma in a reactive-ion plasma system with a low RF power of 50 W and an $O_2$ flow of 50 sccm for 3 min. Sample D was immersed in 5 mM ODT in ethanol at RT for 24 h to passivate the GaN surface. Note that the GaN surface was hydrophilic after HCl cleaning but became hydrophobic during the ODT treatment due to the alkyl termination of the ODT molecule. In order to ensure the GaN surface was passivated by the ODT monolayers in

 

saturation,[14] a 24 h immersion time was used in this study. After ODT exposure, sample D was immersed in ethanol and ultrasonically cleaned for 10 min followed by $N_2$ drying. Furthermore, before ALD, sample D was exposed to 30 cycles of $H_2O$ pulses with the same pulse/purge duration as used in the ALD process at 260 °C in the ALD reactor, to in situ cleave S–C bonds of the ODT SAM. $Al_2O_3$ films with nominal thicknesses of 20 nm were grown by ALD with trimethyl aluminum as the precursor and $H_2O$ as the oxidant source. The 180 ALD cycles were run at 260 °C at a chamber pressure of ~50 Pa. High-purity $N_2$ (20 sccm) was used as the precursor carrier and purge gas. The thickness of $Al_2O_3$ was determined by spectroscopic ellipsometry and found to be close to the nominal value of $20 \pm 0.1$ nm. After local $Al_2O_3$ removal with 1% HF, another photolithography process was used to define the Ni/TiN (50/100 nm) gate electrodes. The GaN surface chemical property was investigated by X-ray photoemission spectroscopy (XPS), and the electrical properties of the MIS devices were measured by using an Agilent B1500A semiconductor analyzer.

## 3. Results and discussion

XPS analysis was conducted to investigate chemical composition variation on the GaN surface induced by the different treatments. XPS measurements were implemented in an AMICUS system consisting of a Mg/Al K$\alpha$ X-ray source and an electron energy analyzer, and the detection depth was expected to be within 5 nm. Moreover, the interval time before the XPS measurement was approximately 8 h. Figure 1 shows the deconvoluted core-level (CL) spectra of Ga 3d for the four samples: no treatment, HCl, $O_2$ plasma and ODT. The C 1s peak of adventitious carbon (284.8 eV) was used for calibration. The XPS data were analyzed after Shirley background subtraction and a Savitzky–Golay smoothing process. The peaks were fitted by using a Gaussian–Lorentzian mixed function. Based on the XPS analysis in Ref. 12, the Ga 3d spectrum can be decomposed as a main component at 19.7 eV related to the Ga–N bonds in the substrate and an additional peak at a higher binding energy (BE; 20.4 eV) associated with the Ga–O bonds. Q2

The Ga 3d spectrum of the non-treated sample in Fig. 1(a) exhibits a high Ga–O sub-peak and this indicates the existence of amorphous native oxide at the $Al_2O_3$/GaN interface. HCl solution is reported to effectively remove native oxide on GaN surfaces;[18] however, the Ga–N and Ga–O bonds' intensities are very similar in Figs. 1(a) and 1(b). The possible reason is that the HCl-treated GaN surface sample was exposed to air before the ALD process, and re-oxidation occurred during this interval. The Ga 3d centroid peak of the $O_2$ plasma treated sample shown in Fig. 1(c) was shifted to a higher BE for approximately 0.2 eV when compared to the non-treated sample. In this case, a broader centroid peak was visible with a larger fitted Ga–O sub-peak. This is mainly due to the GaN cap layer being oxidized and $GaO_x$ forming on the surface.[16] Moreover, the ~0.6 nm GaN cap layer was predicted to be oxidized after the $O_2$ plasma treatment, which was verified by measuring the etching depth on the AlGaN/GaN heterostructure with a multi-cycle digital etching process ($O_2$ plasma followed by 2 M HCl immersion). Hence, it can be deduced that the $O_2$ plasma treatment effectively filled the N vacancies with O atoms, where carrier trapping could be induced. In addition, we noticed a phenomenon where the $O_2$ plasma treatment removed carbon contamination on the GaN, which corresponded to a lower C/N ratio of 1.1, when compared with the value of 1.6 for the ODT-treated sample. Moreover, the S/N ratio for the non-treated sample, the $O_2$ plasma treated sample and the ODT-treated sample was 0.7, 0.7 and 1.3, respectively.

The Ga 3d spectrum of the ODT-treated sample in Fig. 1(d) shows a slightly higher BE of the centroid peak compared to that of the non-treated sample. The fitted Ga–O sub-peak component appears to be reduced indicating the amount of oxide on the GaN surface decreased. There was an extra deconvoluted sub-peak in the Ga 3d CL spectrum at a

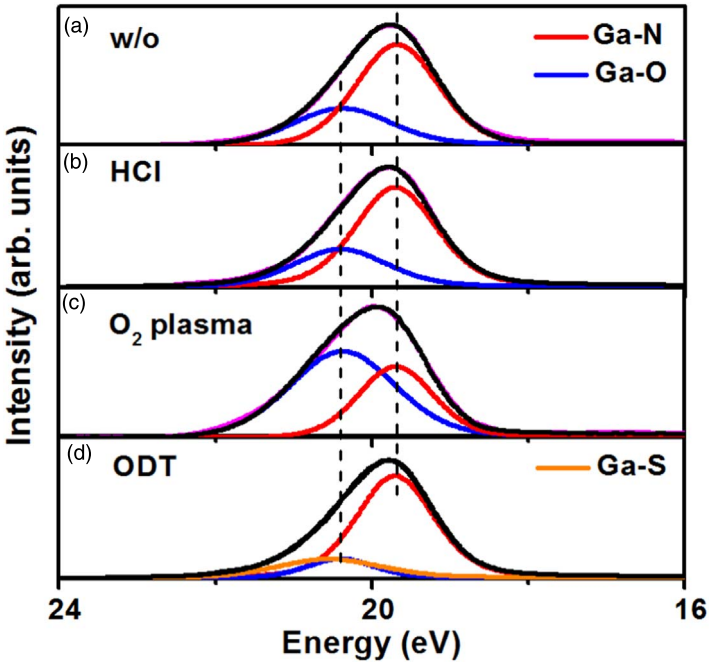


**Fig. 1.** (Color online) The XPS spectra of the Ga 3d CL for the samples: (a) A - without treatment; (b) B - with HCl; (c) C - with $O_2$ plasma; (d) D - with ODT treatment for 24 h.

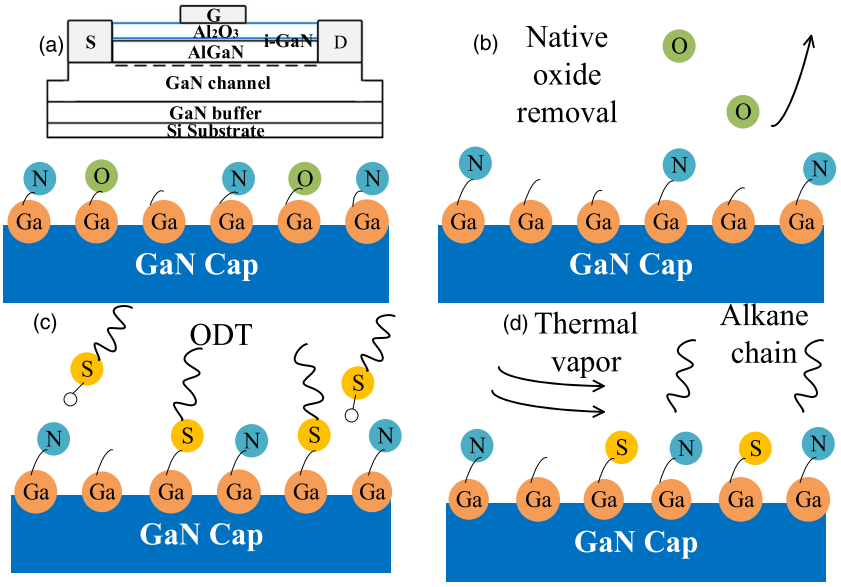


**Fig. 2.** (Color online) Schematic of the ODT treatment procedure: (a) the non-treated GaN cap; (b) the HCl treatment removal of the native oxide; (c) the formation of a dense ODT SAM on the HCl-cleaned GaN surface; (d) the in vacuo thermal vapor removal of the C chain, leaving S atoms behind.

BE of 20.6 eV, which corresponds to bond formation between Ga and S atoms.[12] This suggests that ODT treatment can suppress the oxidation of the GaN surface by forming Ga–S bonds before subsequent $Al_2O_3$ deposition. Furthermore, the Ga–S bonds remained at the surface after exposure to thermal $H_2O$ vapor pulses during ALD. This indicates that the Ga–S bonds were thermally stable at least up to 260 °C, in agreement with previous studies,[19] suggesting that Ga–S bonds remain stable up to 400 °C. Hence, it can be deduced from the XPS study that an ODT self-assembled monolayer is capable of providing good passivation of the GaN surface even during a high-temperature fabrication process, and this feature could allow integration of ODT treatment into the MOSFET process flow.

Figure 2 shows a schematic of the chemical composition on the GaN surface during the ODT treatment. Firstly, wet chemical etching in 2 M HCl was used to remove native oxide on the GaN wafer [Fig. 2(b)]. Secondly, by immersing the wafer in ODT solution at RT for 24 h, the GaN surface was left with the ODT SAM [Fig. 2(c)]. The presence of chemisorbed Ga–S bonds on the GaN surface depicted in the schematic in Fig. 2(c) can be proven by the XPS results and the clear signature of a Ga–S sub-peak shown in Fig. 1(d). Thirdly, the exposure of the surface to $H_2O$ vapor at 260 °C in the ALD reactor led to the removal of the alkane chain of the ODT SAM. This alkane chain reduction may be attributed to the thermal cleavage of S–C bonds.[14] Finally, the Ga–S bonds on the GaN surface acted as a barrier to suppress Ga–O bond formation during the subsequent $Al_2O_3$ deposition [Fig. 2(d)], which could result in a high-quality interface between the ALD-$Al_2O_3$ and the GaN cap.

The multi-frequency $C$–$V$ characteristics of the MIS capacitors at RT (~25 °C) are shown in Fig. 3. The measurement gate voltage ($V_G$) was swept from −14 V to 5 V with a step of 20 mV, and the frequency was varied from 2 MHz down to 1 kHz. The $C$–$V$ curves feature two rising edges. The first rising edge at negative $V_G$ corresponds to the formation of a two-dimensional electron gas (2DEG) channel, and the second rising edge at positive $V_G$ refers to the spill-over of the 2DEG at the $Al_2O_3$/GaN interface.[20] Frequency dispersion at the second rising edge was observed in all samples and a larger frequency dispersion indicated a higher $Al_2O_3$/GaN interface trap density.[21] Furthermore, when applying a higher positive gate bias, electrons started to distribute in the barrier AlGaN layer, leading to the increase of capacitance to the $Al_2O_3$ capacitance. Note that the capacitance of the $O_2$ plasma treated sample C was slightly lower than that of the other three samples. This is likely due to a thin oxidized $GaO_x$ interlayer forming between $Al_2O_3$ and the GaN cap after the $O_2$ plasma treatment, leading to an increase of the equivalent thickness of the gate dielectric. Obvious horizontal frequency dispersion was detected in the second rising edge for samples A, B and C. In contrast, by using ODT GaN surface treatment (sample D), a rising edge with a smaller frequency dispersion was observed.

The $Al_2O_3$/GaN interface trap density can be calculated by the second slope onset voltage ($V_{ON}$) in the $C$–$V$ curves.[22] Note that, when $V_G$ is lower than $V_{ON}$, interface traps at the Fermi level are empty because they are too deep to respond to the ac signal. When $V_G$ increases to $V_{ON}$, interface traps at the Fermi level can respond to the ac signal by capturing or emitting electrons because the interface trap frequency is higher than the ac measurement frequency. Onset voltage dispersion ($\Delta V_{ON}$) occurs at two measurement frequencies ($f_1, f_2$) due to interface traps existing in the energy range from $E_{Trap}(f_1)$ to $E_{Trap}(f_2)$. The detectable energy of the interface trap $E_{Trap}(f_m)$ as a function of the measurement frequency $f_m$ can be represented by:

$$E_{Trap}(f_m) = E_C - E_T = kT \ln\left(\frac{v_{th}\sigma_n N_c}{2\pi f_m}\right) \quad (1)$$

where $k$ is the Boltzmann constant, $T$ is the measurement temperature, $N_c = 2.7 \times 10^{18}\,cm^{-3}$ is the effective density of states in the conduction band of GaN, $\sigma_n$ is the electron capture cross section, and $v_{th} = 2 \times 10^7\,cm\,s^{-1}$ is the thermal velocity of electrons. An equivalent average energy level of

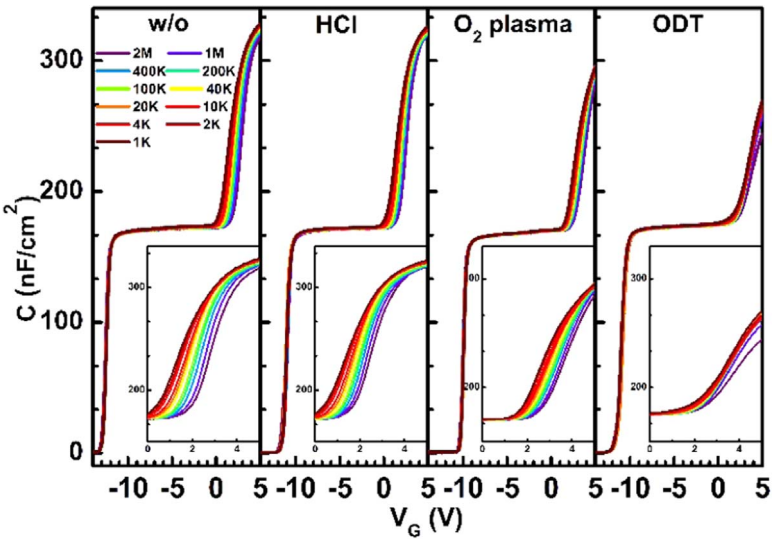


**Fig. 3.** (Color online) Multi-frequency *C–V* characteristics of ALD-$Al_2O_3$/GaN/AlGaN/GaN MIS capacitor structures without treatment (sample A) and with HCl (sample B), $O_2$ plasma (sample C) and ODT (sample D) surface passivation treatments.

the interface state ($E_{AVG}$) in the energy range from $E_{Trap}(f_1)$ to $E_{Trap}(f_2)$ can be found as:

$$E_{AVG} = \frac{E_{Trap}(f_1) + E_{Trap}(f_2)}{2}. \quad (2)$$

According to the interface state density–energy level mapping method proposed by Yang et al.,[23] the distribution of $Al_2O_3$/GaN interface states can be obtained by Eq. (3):

$$D_{it}(E = E_{AVG}) = \frac{C_{OX} \cdot \Delta V_{ON}}{q\Delta E_{Trap}} - \frac{C_{OX} + C_B}{q^2} \quad (3)$$

where $C_{OX}$ is the capacitance of the ALD-$Al_2O_3$ dielectric, $C_B$ is the capacitance of the AlGaN barrier layer, $\Delta E_{Trap}$ is the interface trap frequency-dependent energy difference, and $\Delta V_{ON}$ is the onset voltage frequency-dependent shift ($V_{ON}$ in this study was extracted by reading the voltage when the capacitance reached 110% of the first plateau capacitance). The value of $C_{OX}$ can be extracted as the maximum capacitance observed in the *C–V* plots in Fig. 3, and was found to be 326 nF cm$^{-2}$ for the non-treated samples. It is worth noting that the permittivity of the $Al_2O_3$ film in this study was estimated as ~7.5, which is lower than the expected theoretical value (~9). This is because $Al_2O_3$ deposited by thermal ALD has a lower mass density due to the incorporation of OH groups into the $Al_2O_3$ film.[24] The maximum capacitances were extracted from the *C–V* curves at 1 kHz to avoid the low-frequency limit effect.[25] The barrier layer capacitance can be calculated from the first plateau capacitance in Fig. 3, as the latter refers to the series capacitance connection between $C_{OX}$ and $C_B$. The energy difference of interface states $\Delta E_{Trap}$ is described by Eq. (4)[23] and can be calculated as:

$$\Delta E_{Trap} = E_{Trap}(f_1) - E_{Trap}(f_2). \quad (4)$$

The frequency-dependent shift of onset voltage $\Delta V_{ON}$ can be extracted using Eq. (5):

$$\Delta V_{ON} = V_{ON}(f_1) - V_{ON}(f_2). \quad (5)$$

Figure 4 shows the results of the interface trap density distribution at the $Al_2O_3$/GaN interface for the MIS capacitor

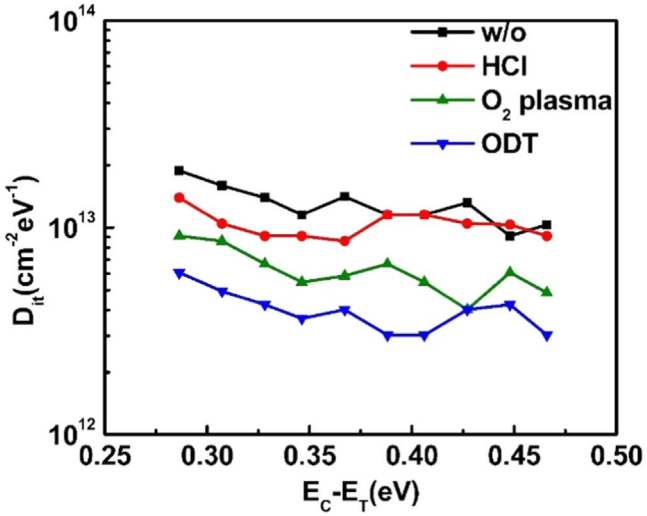


**Fig. 4.** (Color online) Distribution of $D_{it}$ versus ($E_C$–$E_T$) at an ALD-$Al_2O_3$/GaN interface for four types of GaN surface treatments extracted from *C–V* characteristics and Eq. (3).

structures obtained from Eq. (3) and the *C–V* method described above. The electron capture cross section at the interface $\sigma_n$ was assumed to be $1 \times 10^{-14}$ cm$^2$, giving values of $D_{it}$ in the energy level range of ~0.28 eV to ~0.47 eV from the conduction band. For the HCl-treated sample, the extracted $D_{it}$ was calculated to be over $9 \times 10^{12}$ cm$^{-2}$ eV$^{-1}$ in this energy range, which is close to the value of $1.3 \times 10^{13}$ cm$^{-2}$ eV$^{-1}$ reported in another study.[26] This is likely due to the re-oxidation of the exposed GaN surface before the transfer of the sample into the ALD chamber. For the $O_2$ plasma treated sample, $D_{it}$ varied from $9.1 \times 10^{12}$ cm$^{-2}$ eV$^{-1}$ to $4.8 \times 10^{12}$ cm$^{-2}$ eV$^{-1}$, when the energy level depth changed from 0.28 eV to 0.47 eV. In comparison, the ODT-treated sample showed the lowest $D_{it}$ distribution among the four samples from $6.1 \times 10^{12}$ cm$^{-2}$ eV$^{-1}$ down to $3 \times 10^{12}$ cm$^{-2}$ eV$^{-1}$. The reduction of the interface state density can be explained by the ability of the ODT treatment to fill in N vacancies by creating Ga–S bonds, and hence by suppressing re-oxidation which can occur before the ALD process. Meanwhile, surface damage was minimized for the wet treatment; however, $O_2$ plasma treatment may cause GaN

**Table I.** A summary of $D_{it}$ values at $E_C - E_T = \sim 0.47$ eV for the $Al_2O_3$/GaN interfaces from this work and state-of-the-art literature.

| References | 9 | 23 | 27 | 26 | 21 | 28 | 29 | 30 | This work | This work |
|---|---|---|---|---|---|---|---|---|---|---|
| Dielectric | $Al_2O_3$ | $Al_2O_3$ | $Al_2O_3$ | $Al_2O_3$ | $Al_2O_3$ | $Al_2O_3$ | $Al_2O_3$ | $Al_2O_3$ | $Al_2O_3$ | $Al_2O_3$ |
| Deposition technique | PEALD | PEALD | ALD | MOCVD | ALD | ALD | ALD | ALD | ALD | ALD |
| Treatment | In situ $NH_3$/Ar/$N_2$ plasma | In situ $NH_3$/Ar/$N_2$ plasma | UV/ozone | HCl | $N_2O$ plasma | In situ Ar plasma | FG plasma | $N_2$/$O_2$ plasma | ODT | $O_2$ plasma |
| $D_{it} \times 10^{12}$ cm$^{-2}$ eV$^{-1}$ | ~1 | ~2.2 | ~4.1 | ~7 | ~9 | ~30 | ~30 | ~38 | 3.0 | 4.8 |

surface damage and lead to defects in the $Al_2O_3$/GaN interface as shown in this work with relevant results also reported in the literature. Table I benchmarks the $D_{it}$ results in this work with state-of-the-art reported values, where $D_{it}$ refers to the energy level of $E_C - E_T = \sim 0.47$ eV. Note that the $Al_2O_3$/GaN interface state density obtained by using ODT treatment is close to that reported in another study,[9] which is a fairly low interface state density compared with other up-to-date reported data.[21,23,26–30] Furthermore, the cost and complexity of using ODT treatment are much lower than those of in situ $NH_3$/Ar/$N_2$ plasma treatment with a plasma-enhanced ALD-$Al_2O_3$ gate dielectric.

The dc transfer and gate leakage characteristics for the four samples are shown in Fig. 5. The breakdown voltage of the gate dielectric was defined as the gate voltage when the gate current reached 1 $\mu$A mm$^{-1}$. It can be observed that the gate breakdown voltages for samples A, B, C and D were 10.1 V, 11.1 V, 13.2 V and 12.5 V, respectively. The highest breakdown electric field of 6.6 MV cm$^{-1}$ was obtained for the $O_2$ plasma treated sample. The latter can be attributed to the formation of a thin oxidized GaN layer in the gate region.[17] An increase of the actual gate dielectric thickness can also be substantiated from the decrease of the capacitance visible for the $O_2$ plasma treated sample in Fig. 3 and the increased intensity of the Ga–O component from the XPS Ga 3d CL fitting shown in Fig. 1(c). Here, the breakdown characteristic for the ODT-treated sample slightly improved from that of the HCl-treated sample, but was not as good as that for the $O_2$ plasma treated sample. The threshold voltages ($V_{Th}$) of samples A, B, C and D were extracted to be −13.1 V, −11.8 V, −10.4 V, and −12.3 V, respectively, with a drain current criterion of 1 $\mu$A mm$^{-1}$. Compared with that of sample A without surface treatment, $V_{Th}$ shifted towards the positive direction for samples B, C and D likely due to the reduction of positive charges on the treated GaN surface prior to the formation of $Al_2O_3$. The presence of positive charges can be explained as Ga dangling bonds on the GaN surface acting as positive charge centers, generated due to N diffusing and leaving the Ga–N bonds.[31] A more positive $V_{Th}$ of the $O_2$ plasma treated sample was observed, and the reduction of positive charges indicates $O_2$ plasma can passivate N vacancies at $Al_2O_3$/GaN interfaces effectively.

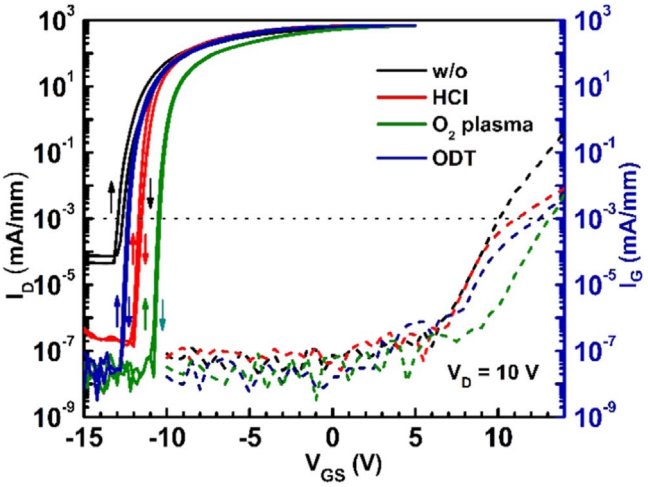


**Fig. 5.** (Color online) Dc $I_D$–$V_{GS}$ and $I_G$–$V_{GS}$ characteristics of the MIS-HEMTs with four types of surface treatments.

The $I_{ON}/I_{OFF}$ ratios of the four samples A, B, C and D were estimated to be $\sim 7 \times 10^6$, $\sim 2 \times 10^9$, $\sim 10^{10}$, and $\sim 10^{10}$, respectively. For the samples with ODT and $O_2$ plasma treatments, the off-state leakage current was suppressed by over three orders of magnitude as compared to that of the sample without treatment. This suggests that N vacancies and impurities on GaN can be reduced by ODT and $O_2$ plasma treatments, hence causing suppressed leakage components through the mesa isolation surface and gate dielectric. Samples A and B exhibited a threshold hysteresis ($\Delta V_{Th}$) of ∼0.3 V and ∼0.18 V, and a subthreshold slope (SS) of ∼150 mV dec$^{-1}$ and ∼100 mV dec$^{-1}$, respectively, revealing a higher interface trap density at the $Al_2O_3$/GaN interface. In contrast, a small $\Delta V_{Th}$ of ∼0.12 V as well as a small SS of ∼73 mV dec$^{-1}$ was observed for the ODT-treated sample. The latter is another evidence that interface traps were suppressed effectively by the ODT treatment. The $O_2$ plasma treated sample also exhibited a reduced $\Delta V_{Th}$ of ∼0.10 V and a reduced SS of ∼68 mV dec$^{-1}$, which are slightly smaller than those of the ODT-treated sample. This indicates that $O_2$ plasma treatment can effectively suppress interface trap related switching transients in MIS-HEMTs. It is worth noting that as a dry process, $O_2$ plasma treatment has relatively high demands for experimental equipment. Among the three treatments, the low-cost ODT treatment demonstrated remarkably improved gate control characteristics of the associated MIS-HEMTs with an increased $I_{ON}/I_{OFF}$ ratio, a reduced $\Delta V_{Th}$ and a reduced SS. Note that the variation of $I_D$–$V_{DS}$ curves for the four samples was not found to be obvious; hence output characteristics for the samples were excluded from this paper.

To assess the $V_{Th}$ stability of the fabricated MIS-HEMTs, a gate bias of 5 V was applied on the devices with both drain and source grounded, and the change of transfer characteristics was monitored. With a gate bias of 5 V, the corresponding electric field in the $Al_2O_3$ gate dielectric layer was approximately 2.5 MV cm$^{-1}$. The total bias time was fixed at 21 000 s. The threshold voltage, $V_{Th}$, shift was monitored by an $I_D$–$V_{GS}$ measurement ($-15\ V < V_{GS} < 5\ V$ and $V_{DS} = 10$ V) after certain bias time intervals (0, 1, 2.1, 4.6, 10, 21, 46, 100, 210, 460, 1000, 2100, 4600, 10 000, and 21 000 s). Figure 6 shows the multiple $I_D$–$V_{GS}$ curves during the 21 000 s gate bias. A positive $V_{Th}$ shift was observed for all samples after the forward bias stress. When the gate bias was sufficiently positive, the high-field regime promoted the conduction of electrons from the GaN interface through the gate dielectric to the gate metal. This phenomenon possibly led to charge trapping at the $Al_2O_3$/GaN interface, and at pre-existing $Al_2O_3$ bulk traps close to the interface,[32] causing detrimental effects reflected in the positive shift of $V_{Th}$. A much larger shift of $I_D$–$V_{GS}$ curves was observed for samples A and B, while the transfer characteristic for sample C with $O_2$ plasma treatment showed good behavior as shown in Fig. 6(c). The subthreshold characteristic of the ODT-treated sample shows suppressed degeneration during the 21 000 s gate bias in Fig. 6(d). Note that the shift of the $I_D$–$V_{GS}$ curve of sample D was still larger than that of sample C after the stress time was increased.

The threshold voltages and their shifts during the 21 000 s gate bias time for the four samples are shown in Figs. 7(a) and 7(b). A bias time dependent shift of $V_{Th}$ to even more

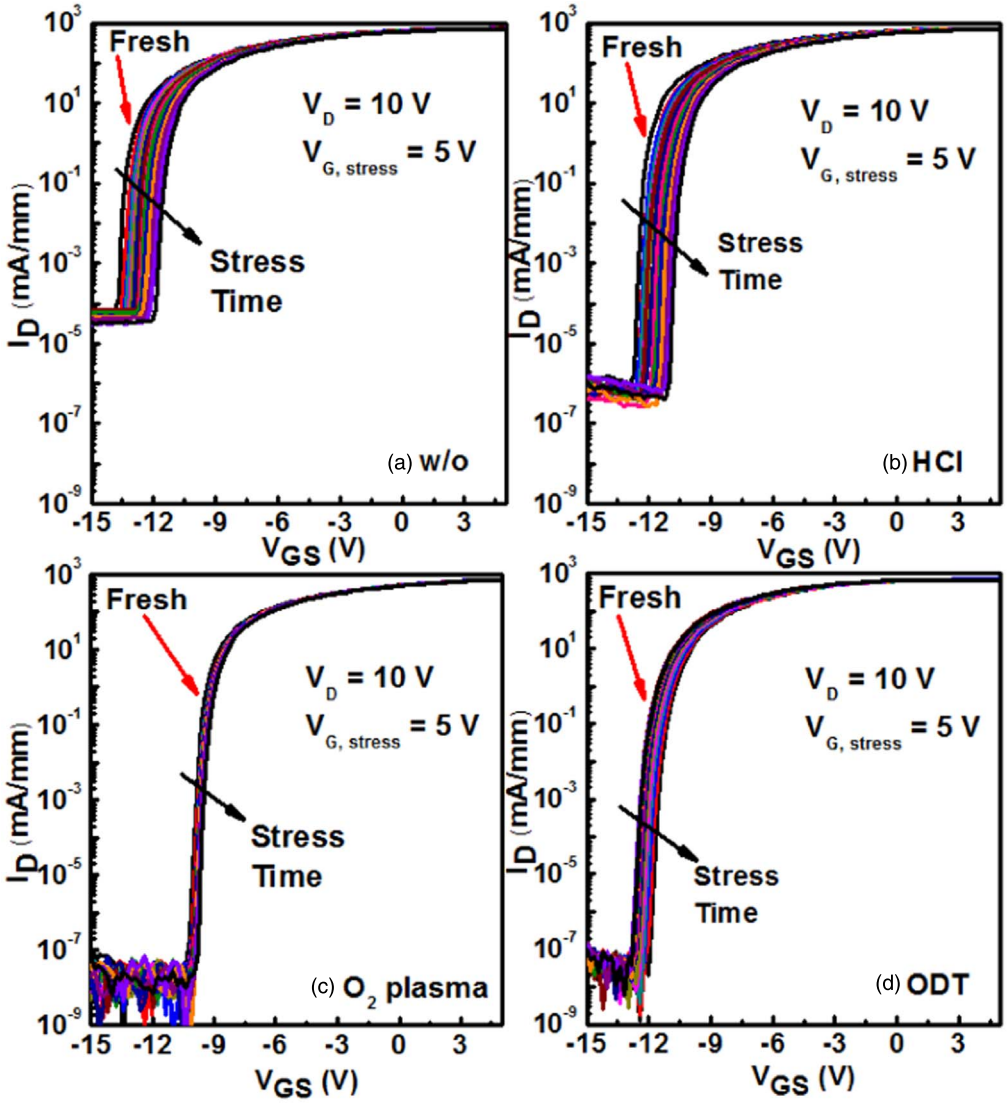


**Fig. 6.** (Color online) Transfer characteristic curves measured during the 21 000 s gate bias: (a) non-treated; (b) HCl, (c) $O_2$ plasma and (d) ODT surface-treated MIS-HEMTs.

positive values was observed for all samples. The $V_{Th}$ shift process consisted of an initial large $V_{Th}$ shift after a 1 s positive gate stress followed by a more gradual $V_{Th}$ shift when the bias time increased to 21 000 s. These observations can be explained by a rapid occupation of interfacial traps occurring initially, followed by a much slower tunneling of electrons to the dielectric bulk traps.[33,34] The sample with ODT treatment showed a relatively small initial $V_{Th}$ shift ($\sim$0.1 V) when compared to the other three samples. This indicates that the $Al_2O_3$/GaN interface trap density was reduced significantly by the ODT treatment. This finding can be further underpinned by the distribution of interface traps extracted by the *C–V* method as shown in Fig. 5. In addition, the $O_2$ plasma treated sample showed a reduced $V_{Th}$ shift of $\sim$0.5 V with a further increase in bias duration compared to samples A, B, and D. Since the surface treatments had a limited effect on the bulk properties of the gate dielectric, the bulk trap density was likely similar for all samples. The $O_2$ plasma treatment was able to fill N vacancies on GaN and break the original Ga–N bond to form a stronger bond of Ga–O.[35] It is possible that the $O_2$ plasma treated interface was more stable with electrical stressing, and thus sample C exhibited a reduced $V_{Th}$ shift. To gain a better understanding of the electron transfer mechanism, negative bias $V_{Th}$ instability measurement and continuous recovery measurement are required to be performed in further research. Q6

## 4. Conclusions

In this paper, surface treatments prior to ALD-$Al_2O_3$ deposition on a GaN/AlGaN/GaN heterostructure have been investigated. An emerging GaN surface passivation process based on ODT treatment has been proposed to improve the $Al_2O_3$/GaN interface quality. The GaN surface was also treated by HCl and $O_2$ plasma. According to the XPS results, re-oxidation is hard to avoid on a HCl-treated GaN surface. In addition, $O_2$ plasma treatment is able to fill N vacancies on the GaN surface with O atoms. Moreover, ODT treatment can passivate N vacancies with S atoms and prevent the formation of detrimental native oxide. The multi-frequency *C–V* results indicate that the ODT treatment reported here is a useful process to reduce the $Al_2O_3$/GaN interface state density. In addition, the *I–V* characteristics indicate that $O_2$ plasma treatment is capable of reducing positive charges on

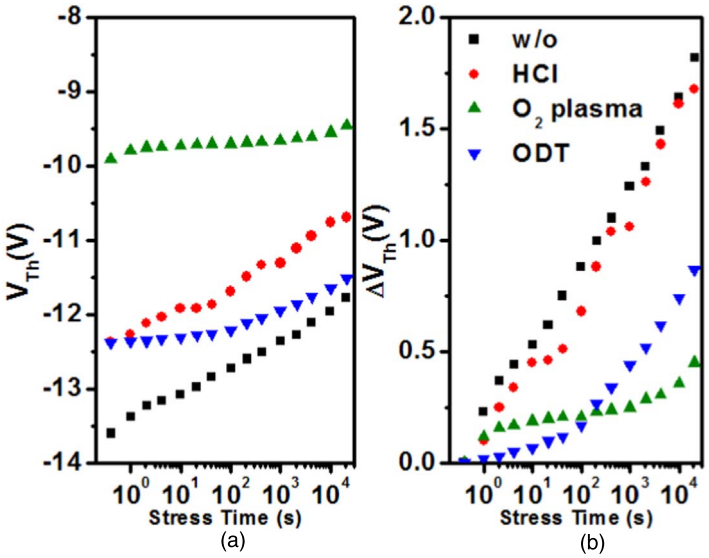


**Fig. 7.** (Color online) (a) The measured threshold voltage, $V_{Th}$, and (b) its shift, $\Delta V_{Th}$, during the 21 000 s gate bias time for the four MIS-HEMT devices.

the GaN surface and of reducing positive bias induced $V_{Th}$ instability considerably. The MIS-HEMTs fabricated using the low-cost ODT GaN surface treatment have been found to exhibit effective characteristics which are highly desirable in power switching applications, such as a low $V_{Th}$ hysteresis of 0.12 V, a small SS of 73 mV dec$^{-1}$, and a high on/off ratio of $10^{10}$.

## Acknowledgments

This work was supported by the Suzhou Science and Technology Program (SYG201728 and SYG201923), Suzhou Industrial Park Initiative Platform Development for the Suzhou Municipal Key Lab for New Energy Technology (RR0140), the Key Program Special Fund in XJTLU (KSF-A-05 and KSF-T-07), and the XJTLU Research Development Fund (PGRS-13-03-01 and RDF-14-02-02).

## ORCID iDs

Yutao Cai https://orcid.org/0000-0002-2151-9325
Ruize Sun https://orcid.org/0000-0003-1884-7114

1) J. J. Freedsman, T. Kubo, and T. Egawa, IEEE Trans. Electron Devices **60**, 3079 (2014).
2) T.-E. Hsieh et al., IEEE Electron Device Lett. **35**, 732 (2015).
3) T. Kubo and T. Egawa, Semicond. Sci. Technol. **32**, 125016 (2017).
4) Y. S. Chiu et al., Jpn. J. Appl. Phys. **55**, 051001 (2016).
5) M. Hatano, Y. Taniguchi, S. Kodama, H. Tokuda, and M. Kuzuhara, Appl. Phys. Express **7**, 044101 (2014).
6) J. Robertson and B. Falabretti, J. Appl. Phys. **100**, 014111 (2006).
7) D. Hoogeland, K. Jinesh, F. Roozeboom, W. Besling, M. Van De Sanden, and W. Kessels., J. Appl. Phys. **106**, 114107 (2009).
8) M. Ťapajna et al., J. Appl. Phys. **116**, 104501 (2014).
9) S. Liu et al., Appl. Phys. Lett. **106**, 051605 (2015).
10) E. Schilirò, P. Fiorenza, G. Greco, F. Roccaforte, and R. Lo Nigro, J. Vac. Sci. Technol. A **35**, 01B140 (2017).
11) T. Hossain et al., J. Vac. Sci. Technol. B **33**, 061201 (2015).
12) A. Kumar, T. Singh, M. Kumar, and R. Singh, Curr. Appl. Phys. **14**, 491 (2013).
13) É. O'Connor et al., J. Appl. Phys. **109**, 024101 (2011).
14) D. Cuypers et al., Chem. Mater. **28**, 5689 (2016).
15) J. Dorsten, J. Maslar, and P. Bohn, Appl. Phys. Lett. **66**, 1755 (1995).
16) R. Stoklas et al., Semicond. Sci. Technol. **32**, 045018 (2017).
17) M. Hua et al., IEEE Electron Device Lett. **38**, 929 (2017).
18) S. King et al., J. Appl. Phys. **84**, 5248 (1998).
19) A. Islam, T. Tambo, and C. Tatsuyama, J. Appl. Phys. **85**, 4003 (1999).
20) Z. Yatabe et al., Jpn. J. Appl. Phys. **53**, 100213 (2014).
21) Y. Hori, Z. Yatabe, and T. Hashizume, J. Appl. Phys. **114**, 244503 (2013).
22) N. Ramanan, B. Lee, and V. Misra, IEEE Trans. Electron Devices **62**, 546 (2014).
23) S. Yang, S. Liu, Y. Lu, C. Liu, and K. J. Chen, IEEE Trans. Electron Devices **62**, 1870 (2015).
24) J. T. Gaskins et al., ECS J. Solid State Sci. Technol. **6**, 189 (2017).
25) M. Capriotti et al., J. Appl. Phys. **117**, 024506 (2015).
26) M. Ťapajna et al., Appl. Surf. Sci. **426**, 656 (2017).
27) K. Kim, Electron. Mater. Lett.~~(in press)~~. Q7
28) Z. Zaidi, K. Lee, J. Roberts, I. Guiney, H. Qian, S. Jiang, J. Cheong, P. Li, D. Wallis, and C. Humphreys, J. Appl. Phys. **123**, 184503 (2018).
29) X. Qin, A. Lucero, A. Azcatl, J. Kim, and R. M. Wallace, Appl. Phys. Lett. **105**, 011602 (2014).
30) X. Qin, H. Dong, J. Kim, and R. M. Wallace, Appl. Phys. Lett. **105**, 141604 (2014).
31) L. Shen et al., IEEE Electron Device Lett. **38**, 596 (2017).
32) T.-L. Wu et al., Appl. Phys. Lett. **107**, 093507 (2015).
33) Y. Lu, S. Yang, Q. Jiang, Z. Tang, B. Li, and K. J. Chen, Phys. Status Solidi C **10**, 1397 (2013).
34) P. Lagger, M. Reiner, D. Pogany, and C. Ostermaier., IEEE Trans. Electron Devices **61**, 1022 (2014).
35) G. Martinez, M. Curiel, B. Skromme, and R. Molnar, J. Electron. Mater. **29**, 325 (2000).

 